

## Supporting Information

### Highly Stable and Reversible Birefringent Switching Triggered by Thermally Stimulated Phase Transition

Cheng Chen,<sup>a</sup> Yunjie Bai,<sup>a</sup> Qi Shi,<sup>a</sup> Mingye Han,<sup>a</sup> Bingbing Zhang,<sup>ab</sup> Ying Wang<sup>ab\*</sup>

<sup>a</sup> College of Chemistry and Materials Science, Hebei Research Center of the Basic Discipline of Synthetic Chemistry, Key Laboratory of Medicinal Chemistry and Molecular Diagnosis of the Ministry of Education, Key Laboratory of Chemical Biology of Hebei Province, Hebei University, Baoding 071002, China. Email: wangy@hbu.edu.cn

<sup>b</sup> Institute of Life Science and Green Development, Hebei University, Baoding 071002, China.

### Table of Contents

#### Experimental and Theoretical Calculation Details

**Table S1.** Crystal data and structure refinements for the  $P\bar{1}$  phase and  $P2_1/c$  phase of  $KCe(SO_4)_2$ .

**Table S2.** Atomic coordinates and equivalent isotropic displacement parameters for the  $P\bar{1}$  phase of  $KCe(SO_4)_2$ .

**Table S3.** Atomic coordinates and equivalent isotropic displacement parameters for  $P2_1/c$  phase of  $KCe(SO_4)_2$ .

**Table S4.** Bond lengths [Å] for the  $P\bar{1}$  phase of  $KCe(SO_4)_2$ .

**Table S5.** Bond angles [deg] for the  $P\bar{1}$  phase of  $KCe(SO_4)_2$ .

**Table S6.** Bond lengths [Å] for the  $P2_1/c$  phase of  $KCe(SO_4)_2$ .

**Table S7.** Bond angles [deg] for the  $P2_1/c$  phase of  $KCe(SO_4)_2$ .

**Table S8.** The thermal stability, birefringent variation and number of cycles of the reported materials caused by phase transitions.

**Table S9.** Local dipole moment calculation for the  $P\bar{1}$  phase of  $KCe(SO_4)_2$ .

**Table S10.** Local dipole moment calculation for the  $P2_1/c$  phase of  $KCe(SO_4)_2$ .

**Figure S1.** The fundamental building unit of the (a)  $P\bar{1}$  phase of  $KCe(SO_4)_2$  and the [Ce-S-O] chain of the (b)  $P2_1/c$  phase of  $KCe(SO_4)_2$ .

**Figure S2.** The *in-situ* variable-temperature PXRD patterns of  $P\bar{1}$ - $KCe(SO_4)_2$ .

**Figure S3.** The elemental analysis results for the  $P\bar{1}$  phase and  $P2_1/c$  phase of  $KCe(SO_4)_2$ .

**Figure S4.** IR Spectra of (a)  $P\bar{1}$  phase and (b)  $P2_1/c$  phase of  $KCe(SO_4)_2$ .

**Figure S5.** UV-vis-NIR diffuse reflectance spectra of (a)  $P\bar{1}$  phase and (b)  $P2_1/c$  phase of  $KCe(SO_4)_2$ .

**Figure S6.** The calculated and experimental values of birefringence of (a)  $P\bar{1}$  phase and (b)  $P2_1/c$  phase of  $KCe(SO_4)_2$ .

**Figure S7.** The measurement of thickness of (a)  $P\bar{1}$  phase and (b)  $P2_1/c$  phase of  $KCe(SO_4)_2$ .

**Figure S8.** Comparison of (a) original and (b) achieved extinction images of the crystal after the phase transition of  $P\bar{1}$ - $KCe(SO_4)_2$ .

**Figure S9.** The calculated band gaps of (a)  $P\bar{1}$  phase and (b)  $P2_1/c$  phase of  $KCe(SO_4)_2$ .

#### Reference

### **Experimental and Theoretical Calculation Details:**

**Reagents.** K<sub>2</sub>SO<sub>4</sub> (99%, Aladdin Chemical Industry Co., Ltd.), sulfuric acid (H<sub>2</sub>SO<sub>4</sub>, 98%, Beijing Chemical Reagent Co., Ltd.) and CeO<sub>2</sub> (99.999%, Hawkhi Science and technology Co., Ltd.) were used without further processing.

**Synthesis.** The single crystals of the the *P* and *P*2<sub>1</sub>/c - KCe(SO<sub>4</sub>)<sub>2</sub> were synthesized via conventional hydrothermal method under the same condition but with different ratios of raw materials. For *P* phase, CeO<sub>2</sub> (0.1033g, 0.6 mmol), K<sub>2</sub>SO<sub>4</sub> (0.2614g, 1.5 mmol), H<sub>2</sub>SO<sub>4</sub> (0.2 ml) were combined with 2 mL deionized water. The concentration of sulfuric acid is 1.67 mol/L. For *P*2<sub>1</sub>/c phase of KCe(SO<sub>4</sub>)<sub>2</sub>, the initial raw materials were CeO<sub>2</sub> (0.1033g, 0.6 mmol), K<sub>2</sub>SO<sub>4</sub> (0.2614g, 1.5 mmol), H<sub>2</sub>SO<sub>4</sub>(0.5 ml), and deionized water (1.0 mL). The concentration of sulfuric acid is 6.13 mol/L. The mixture was placed in a 23 mL Teflon-lined autoclave and then sealed. The autoclave was heated to 230 °C within 4 h, held at that temperature for 4 days and then cooled to room temperature at a rate of 3 °C/h. After filtering and washing with deionized water to remove the excess acid, pure block-like KCe(SO<sub>4</sub>)<sub>2</sub> crystals were obtained as single phase. The yields of the KCe(SO<sub>4</sub>)<sub>2</sub> polymorph are 30% and 65% (based on CeO<sub>2</sub>), for *P* phase and *P*2<sub>1</sub>/c phase, respectively.

**Single-Crystal Structure Determination.** Single-crystal data for the *P* and *P*2<sub>1</sub>/c - KCe(SO<sub>4</sub>)<sub>2</sub> were collected on a Bruker D8 VENTURE diffractometer equipped with a Mo IμS 3.0 microfocus X-ray source ( $\lambda = 0.71073 \text{ \AA}$ ). Integration and absorption correction of the single-crystal data was performed using the SAINT program and processed by Olex2.<sup>1</sup> The structure was solved using the intrinsic phase method and refined using least squares techniques. The structure was checked for possible higher symmetry using PLATON.<sup>2</sup> Crystal data and detailed refinement information are given in Table S1. Atom positions, isotropic displacement parameters, and bond valence sums of each atom are presented in Tables S2 and S3, for the *P* phase and *P*2<sub>1</sub>/c phase of KCe(SO<sub>4</sub>)<sub>2</sub>, respectively. Selected bond distances and angles are summarized in Tables S4-S7.

**Powder XRD.** Powder XRD was measured on a Haoyuan DX-27 mini X-ray diffractometer with Cu K $\alpha$  radiation ( $\lambda = 1.54056 \text{ \AA}$ ) at room temperature. The scanning was done with the 2θ angles in the interval of 5–70°, a scan step width of 0.02°, and a fixed counting time of 2 s.

**Thermal Analysis.** The thermal gravimetric (TG) analysis and differential scanning calorimetry (DSC) of *P* and *P*2<sub>1</sub>/c - KCe(SO<sub>4</sub>)<sub>2</sub> were studied with a HENVEN HCT-2 instrument under flowing air. The sample was placed in an Al<sub>2</sub>O<sub>3</sub> crucible and heated from 30 to 1100 °C with heating rates of 10 °C /min or 5 °C /min.

**Infrared Spectroscopy.** The IR spectra were recorded on a Shimadzu IR Affinity-1 Fourier transform infrared spectrometer in the range of 400–4000 cm<sup>-1</sup>. The sample was mixed with KBr and ground well.

**UV-vis-NIR Diffuse Reflectance Spectrum.** The diffuse reflectance spectrum was measured at room temperature with a Shimadzu UV-2600i UV spectrophotometer in the 200–1400 nm wavelength range.

**Birefringence Measurements.** The birefringence was assessed with a polarizing microscope (NIKON Eclipse Ci-POL) equipped with a Berek compensator under the light source of 546 nm. According to the equation, R (retardation) = Δn × d, the birefringence was calculated, where R, Δn, and d represent the optical path difference, birefringence, and the thickness of crystal, respectively. The thickness of the crystalline sample was measured on a single-crystal XRD diffractometer. Variable temperature birefringence measurement was carried out using a polarizing microscope hot stage from 30 to 300 °C.

**Theoretical Calculations.** The electronic structures and optical properties for *P* and *P*2<sub>1</sub>/c - KCe(SO<sub>4</sub>)<sub>2</sub> were calculated by using the CASTEP package.<sup>3</sup> The generalized gradient approximation

(GGA) with the Perdew–Burke–Ernzerhof (PBE) functional was selected as exchange-correlation potential.<sup>4</sup> The norm-conserving pseudopotentials (NCP) were adopted. The cutoff energy were set as 850 eV for both compounds.<sup>5</sup> The dense  $k$ -points in the Brillouin zone were set as  $1 \times 1 \times 1$ , for the  $P\bar{I}$  phase and  $P2_1/c$  phase of  $\text{KCe}(\text{SO}_4)_2$ , respectively. The configurations for diverse electron orbital were K:  $3s^23p^64s^1$ , Ce:  $4f^15d^16s^2$ , S:  $3s^23p^4$  and O:  $2s^22p^4$ . The GGA method usually underestimates the band gaps of crystals; therefore, the HSE06 method was also adopted to evaluate the band gap.<sup>6</sup>

**Table S1.** Crystal data and structure refinements for the  $P\bar{1}$  phase and  $P2_1/c$  phase of  $\text{KCe}(\text{SO}_4)_2$ .

Empirical formula	$\text{KCe}(\text{SO}_4)_2$	
Formula weight	371.34	371.34
Temperature [K]	273.15	273.15
Crystal system	triclinic	monoclinic
Space group (number)	$P\bar{1}$ (2)	$P2_1/c$ (14)
$a$ [\AA]	5.4149(3)	8.5579(9)
$b$ [\AA]	6.9709(3)	7.2112(7)
$c$ [\AA]	8.4674(4)	10.7675(10)
$\alpha$ [ $^\circ$ ]	86.3480(10)	90
$\beta$ [ $^\circ$ ]	88.4250(10)	92.569(4)
$\gamma$ [ $^\circ$ ]	88.5510(10)	90
Volume [\AA <sup>3</sup> ]	318.76(3)	663.82(11)
$Z$	2	4
$\rho_{\text{calc}}$ [g cm <sup>-3</sup> ]	3.869	3.716
$\mu$ [mm <sup>-1</sup> ]	8.454	8.119
$F(000)$	346	692
Radiation	Mo $K_\alpha$ ( $\lambda=0.71073$ \AA)	Mo $K_\alpha$ ( $\lambda=0.71073$ \AA)
2 $\Theta$ range [ $^\circ$ ]	4.82 to 55.05 (0.77 \AA)	4.76 to 54.96 (0.77 \AA)
Index ranges	-7 $\leq h \leq$ 7 -9 $\leq k \leq$ 9 -10 $\leq l \leq$ 10	-11 $\leq h \leq$ 11 -9 $\leq k \leq$ 9 -13 $\leq l \leq$ 1
Reflections collected	27954	32521
Independent reflections	1452	1523
	$R_{\text{int}} = 0.0287$	$R_{\text{int}} = 0.0380$
	$R_{\text{sigma}} = 0.0107$	$R_{\text{sigma}} = 0.0115$
Completeness	99.7 %	100.0 %
Data / Restraints /	1452/0/109	1523/0/109
Parameters		
Goodness-of-fit on $F^2$	1.176	1.136
Final $R$ indexes [ $I \geq 2\sigma(I)$ ] <sup>a</sup>	$R_1 = 0.0130$ , $wR_2 = 0.0324$	$R_1 = 0.0129$ , $wR_2 = 0.0297$
Final $R$ indexes [all data] <sup>a</sup>	$R_1 = 0.0131$ , $wR_2 = 0.0324$	$R_1 = 0.0151$ , $wR_2 = 0.0303$
Largest peak/hole [e\AA <sup>-3</sup> ]	0.46/-0.70	0.34/-0.69

<sup>a</sup>  $R_1 = F_o - F_c/F_o$  and  $wR_2 = [w(F_o^2 - F_c^2)^2/wF_o^4]^{1/2}$  for  $F_o^2 > 2(F_c^2)$ .

**Table S2.** Atomic coordinates and equivalent isotropic displacement parameters for the  $P\bar{1}$  phase of  $\text{KCe}(\text{SO}_4)_2$ .  $U(\text{eq})$  is defined as one-third of the trace of the orthogonalized  $U_{ij}$  tensor.

Atom	x	y	z	$U_{\text{eq}}$	BVS
Ce1	0.31200(3)	0.68038(2)	0.20167(2)	0.00933(5)	3.0
K1	0.74813(12)	1.15431(9)	0.31529(7)	0.01659(12)	1.4
S1	-0.22229(11)	0.80379(9)	-0.04685(7)	0.00833(12)	6.0
S2	0.75915(11)	0.67558(9)	0.43168(7)	0.00864(12)	6.0
O1	-0.3848(4)	0.6445(3)	-0.0841(2)	0.0163(4)	2.0
O2	-0.3297(4)	0.8819(3)	0.0974(2)	0.0149(4)	2.1
O3	-0.2133(4)	0.9505(3)	-0.1779(2)	0.0138(4)	2.0
O4	0.0293(3)	0.7250(3)	-0.0184(2)	0.0140(4)	2.1
O5	0.5385(3)	0.8062(3)	0.4236(2)	0.0118(4)	2.2
O6	0.7313(4)	0.5406(3)	0.3062(2)	0.0157(4)	2.0
O7	0.7701(4)	0.5783(3)	0.5891(2)	0.0164(4)	2.0
O8	0.9846(3)	0.7875(3)	0.3984(2)	0.0144(4)	2.1

**Table S3.** Atomic coordinates and equivalent isotropic displacement parameters for the  $P2_1/c$  phase of  $\text{KCe}(\text{SO}_4)_2$ .  $U(\text{eq})$  is defined as one-third of the trace of the orthogonalized  $U_{ij}$  tensor.

Atom	x	y	z	$U_{\text{eq}}$	BVS
Ce1	0.55906(2)	0.17079(2)	0.34957(2)	0.00822(5)	3.3
K1	1.06250(6)	0.14702(8)	-0.15580(5)	0.01786(11)	1.2
S1	0.77982(6)	0.34318(7)	0.09271(5)	0.00927(10)	6.0
S2	0.31127(6)	0.33272(7)	0.60930(5)	0.00887(11)	6.0
O1	0.80762(19)	0.2509(2)	-0.02668(14)	0.0139(3)	2.0
O2	0.62533(18)	0.4387(2)	0.06637(15)	0.0140(3)	2.2
O3	0.8984(2)	0.4736(2)	0.13070(16)	0.0191(4)	2.0
O4	0.7577(2)	0.2020(2)	0.18988(15)	0.0167(3)	2.0
O5	0.3674(2)	0.3172(2)	0.48351(15)	0.0156(3)	2.1
O6	0.14515(19)	0.3607(2)	0.60795(16)	0.0158(3)	2.0
O7	0.40008(18)	0.4861(2)	0.67494(14)	0.0130(3)	2.1
O8	0.35692(19)	0.1661(2)	0.68715(15)	0.0131(3)	2.0

**Table S4.** Bond lengths [ $\text{\AA}$ ] for the  $P\bar{1}$  phase of  $\text{KCe}(\text{SO}_4)_2$ .

Atom-Atom	lengths	Atom-Atom	lengths
Ce1–K1	4.2828(7)	K1–O3 <sup>#3</sup>	3.267(2)
Ce1–S1 <sup>#1</sup>	3.3339(6)	K1–O4 <sup>#6</sup>	2.845(2)
Ce1–S2	3.1470(6)	K1–O5 <sup>#7</sup>	2.691(2)
Ce1–O1 <sup>#2</sup>	2.549(2)	K1–O5	2.796(2)
Ce1–O1 <sup>#1</sup>	2.907(2)	K1–O6 <sup>#8</sup>	2.689(2)
Ce1–O2 <sup>#1</sup>	2.531(2)	K1–O7 <sup>#9</sup>	3.389(2)
Ce1–O3 <sup>#3</sup>	2.6108(19)	K1–O8 <sup>#9</sup>	2.913(2)
Ce1–O4	2.4434(19)	K1–O8	2.886(2)
Ce1–O5	2.4888(19)	S1–O1	1.489(2)
Ce1–O6	2.603(2)	S1–O2	1.468(2)
Ce1–O7 <sup>#4</sup>	2.4856(19)	S1–O3	1.4612(19)
Ce1–O8 <sup>#5</sup>	2.531(2)	S1–O4	1.4762(19)
K1–S1 <sup>#6</sup>	3.3877(9)	S2–O6	1.476(2)
K1–O1 <sup>#3</sup>	3.064(2)	S2–O7	1.459(2)
K1–O2 <sup>#1</sup>	2.778(2)	S2–O8	1.4763(19)
K1–O3 <sup>#6</sup>	2.844(2)		

Symmetry transformations used to generate equivalent atoms:

#1: 1+X, +Y, +Z; #2: -X, 1-Y, -Z; #3: -X, 2-Y, -Z; #4: -1+X, +Y, +Z; #5: 1-X, 1-Y, 1-Z; #6: 1-X, 2-Y, -Z; #7: 2-X, 2-Y, 1-Z; #8: 1-X, 2-Y, 1-Z; #9: +X, 1+Y, +Z; #10: +X, -1+Y, +Z;

**Table S5.** Bond angles [deg] for the  $P\bar{1}$  phase of  $\text{KCe}(\text{SO}_4)_2$ .

Atom–Atom–Atom	Angle [°]	Atom–Atom–Atom	Angle [°]
S1–Ce1–K1	62.580(14)	O5–Ce1–O1	126.50(6)
S2–Ce1–K1	52.097(14)	O5–Ce1–O1	113.51(6)
S2–Ce1–S1	78.254(16)	O5–Ce1–O2	69.29(6)
O1–Ce1–K1	137.23(5)	O5–Ce1–O3	76.18(6)
O1–Ce1–K1	89.05(4)	O5–Ce1–O6	55.24(6)
O1–Ce1–S1	26.49(4)	O5–Ce1–O8	73.95(6)
O1–Ce1–S1	82.14(5)	O6–Ce1–K1	72.40(4)
O1–Ce1–S2	95.30(4)	O6–Ce1–S1	68.92(5)
O1–Ce1–S2	99.84(5)	O6–Ce1–S2	27.75(4)
O1–Ce1–O1	58.96(7)	O6–Ce1–O1	76.25(6)
O1–Ce1–O3	152.51(6)	O6–Ce1–O3	122.03(6)
O1–Ce1–O6	72.79(6)	O7–Ce1–K1	118.52(5)
O2–Ce1–K1	38.22(4)	O7–Ce1–S1	136.77(5)
O2–Ce1–S1	24.43(4)	O7–Ce1–S2	73.74(5)
O2–Ce1–S2	66.02(5)	O7–Ce1–O1	71.19(7)
O2–Ce1–O1	50.84(6)	O7–Ce1–O1	126.31(6)
O2–Ce1–O1	104.90(6)	O7–Ce1–O2	138.35(7)
O2–Ce1–O3	65.86(6)	O7–Ce1–O3	133.58(6)
O2–Ce1–O6	68.50(6)	O7–Ce1–O5	80.17(7)
O2–Ce1–O8	124.73(6)	O7–Ce1–O6	70.96(6)
O3–Ce1–K1	49.64(4)	O7–Ce1–O8	69.03(6)
O3–Ce1–S1	82.72(4)	O8–Ce1–K1	88.74(4)
O3–Ce1–S2	99.36(5)	O8–Ce1–S1	147.49(5)
O3–Ce1–O1	99.79(6)	O8–Ce1–S2	96.64(5)
O4–Ce1–K1	118.68(5)	O8–Ce1–O1	130.17(6)
O4–Ce1–S1	89.08(5)	O8–Ce1–O1	162.97(6)
O4–Ce1–S2	166.87(5)	O8–Ce1–O3	66.29(6)
O4–Ce1–O1	74.14(6)	O8–Ce1–O6	118.98(6)
O4–Ce1–O1	81.62(7)	S1–K1–O7	63.18(4)
O4–Ce1–O2	100.93(6)	O1–K1–S1	92.04(4)
O4–Ce1–O3	75.32(6)	O1–K1–O3	44.93(5)
O4–Ce1–O5	151.38(6)	O1–K1–O7	115.35(5)
O4–Ce1–O6	147.97(6)	O2–K1–S1	74.16(4)
O4–Ce1–O7	118.71(7)	O2–K1–O1	76.06(6)
O4–Ce1–O8	92.19(6)	O2–K1–O3	71.76(6)
O5–Ce1–K1	38.35(4)	O2–K1–O3	54.37(6)
O5–Ce1–S1	89.86(4)	O2–K1–O4	70.48(6)
O5–Ce1–S2	27.50(4)	O2–K1–O5	61.59(6)

O2–K1–O7	135.67(6)	O6–K1–O3	106.20(6)
O2–K1–O8	67.06(6)	O6–K1–O4	74.87(6)
O2–K1–O8	141.92(6)	O6–K1–O5	148.43(6)
O3–K1–S1	116.22(4)	O6–K1–O5	82.19(6)
O3–K1–S1	25.24(4)	O6–K1–O7	56.61(6)
O3–K1–O1	114.86(6)	O6–K1–O8	80.62(6)
O3–K1–O3	124.63(7)	O6–K1–O8	151.76(6)
O3–K1–O4	49.83(5)	O8–K1–S1	99.16(4)
O3–K1–O7	159.41(5)	O8–K1–S1	83.32(4)
O3–K1–O7	64.60(5)	O8–K1–O1	142.02(6)
O3–K1–O8	58.79(6)	O8–K1–O1	142.71(6)
O3–K1–O8	86.49(6)	O8–K1–O3	144.49(6)
O4–K1–S1	25.55(4)	O8–K1–O3	104.97(5)
O4–K1–O1	66.53(6)	O8–K1–O7	95.48(5)
O4–K1–O3	96.47(5)	O8–K1–O7	43.98(5)
O4–K1–O7	75.71(5)	O8–K1–O8	74.97(6)
O4–K1–O8	104.43(6)	Ce1–S1–K1	169.74(2)
O4–K1–O8	118.24(6)	Ce1–S1–K1	78.994(16)
O5–K1–S1	124.53(4)	K1–S1–K1	99.81(2)
O5–K1–S1	161.99(5)	O1–S1–Ce1	60.56(8)
O5–K1–O1	95.78(6)	O1–S1–K1	54.24(8)
O5–K1–O1	106.88(6)	O1–S1–K1	110.39(9)
O5–K1–O2	123.49(6)	O2–S1–Ce1	45.47(8)
O5–K1–O3	80.31(6)	O2–S1–K1	101.94(8)
O5–K1–O3	61.96(5)	O2–S1–K1	143.76(9)
O5–K1–O3	104.94(6)	O2–S1–O1	105.83(12)
O5–K1–O3	148.97(6)	O2–S1–O4	110.60(12)
O5–K1–O4	131.45(6)	O3–S1–Ce1	129.92(8)
O5–K1–O4	155.50(6)	O3–S1–K1	62.05(8)
O5–K1–O5	68.37(7)	O3–S1–K1	56.08(8)
O5–K1–O7	137.01(5)	O3–S1–O1	110.67(12)
O5–K1–O7	98.82(6)	O3–S1–O2	111.32(12)
O5–K1–O8	65.07(6)	O3–S1–O4	109.36(11)
O5–K1–O8	96.31(6)	O4–S1–Ce1	120.20(8)
O5–K1–O8	50.39(5)	O4–S1–K1	56.23(8)
O5–K1–O8	99.83(6)	O4–S1–K1	146.89(8)
O6–K1–S1	86.79(5)	O4–S1–O1	108.99(12)
O6–K1–O1	63.81(6)	Ce1–S2–K1	160.89(2)
O6–K1–O2	134.76(6)	Ce1–S2–K1	81.319(18)
O6–K1–O3	103.14(6)	Ce1–S2–K1	78.447(17)

K1–S2–K1	79.99(2)	S1–O1–K1	102.54(10)
K1–S2–K1	79.74(2)	Ce1–O2–K1	107.46(7)
K1–S2–K1	94.27(2)	S1–O2–Ce1	110.11(11)
O5–S2–Ce1	50.73(8)	S1–O2–K1	142.07(12)
O5–S2–K1	53.26(8)	Ce1–O3–K1	113.80(7)
O5–S2–K1	113.26(8)	Ce1–O3–K1	92.86(6)
O5–S2–K1	39.81(8)	K1–O3–K1	124.63(7)
O6–S2–Ce1	55.17(8)	S1–O3–Ce1	133.78(11)
O6–S2–K1	139.02(8)	S1–O3–K1	98.69(9)
O6–S2–K1	116.54(8)	S1–O3–K1	94.68(9)
O6–S2–K1	124.44(9)	Ce1–O4–K1	115.32(7)
O6–S2–O5	105.90(11)	S1–O4–Ce1	138.07(12)
O7–S2–Ce1	126.44(9)	S1–O4–K1	98.23(9)
O7–S2–K1	69.72(8)	Ce1–O5–K1	108.12(7)
O7–S2–K1	130.71(9)	Ce1–O5–K1	113.01(7)
O7–S2–K1	65.27(9)	K1–O5–K1	111.63(7)
O7–S2–O5	109.47(11)	S2–O5–Ce1	101.77(9)
O7–S2–O6	112.60(12)	S2–O5–K1	101.57(9)
O7–S2–O8	109.79(12)	S2–O5–K1	119.51(10)
O8–S2–Ce1	123.61(8)	Ce1–O6–K1	111.74(7)
O8–S2–K1	122.11(8)	S2–O6–Ce1	97.08(9)
O8–S2–K1	56.72(8)	S2–O6–K1	131.32(11)
O8–S2–K1	46.30(8)	Ce1–O7–K1	110.81(7)
O8–S2–O5	109.66(11)	S2–O7–Ce1	156.30(13)
O8–S2–O6	109.33(12)	S2–O7–K1	91.72(9)
Ce1–O1–Ce1	121.04(7)	Ce1–O8–K1	114.96(7)
Ce1–O1–K1	102.21(7)	Ce1–O8–K1	104.86(6)
Ce1–O1–K1	96.99(6)	K1–O8–K1	105.03(6)
S1–O1–Ce1	92.95(9)	S2–O8–Ce1	120.98(11)
S1–O1–Ce1	134.46(12)	S2–O8–K1	112.21(10)
S2–O8–K1	97.96(9)		

Symmetry transformations used to generate equivalent atoms:

#1: 1+X, +Y, +Z; #2: -X, 1-Y, -Z; #3: -X, 2-Y, -Z; #4: -1+X, +Y, +Z; #5: 1-X, 1-Y, 1-Z; #6: 1-X, 2-Y, -Z; #7: 2-X, 2-Y, 1-Z; #8: 1-X, 2-Y, 1-Z; #9: +X, 1+Y, +Z; #10: +X, -1+Y, +Z;

**Table S6.** Bond lengths [ $\text{\AA}$ ] for the  $P2_1/c$  phase of  $\text{KCe}(\text{SO}_4)_2$ .

Atom-Atom	lengths	Atom-Atom	lengths
Ce1–K1 <sup>#1</sup>	4.4459(7)	K1–O3 <sup>#3</sup>	2.7792(18)
Ce1–S1 <sup>#2</sup>	3.1608(6)	K1–O4 <sup>#9</sup>	2.9815(18)
Ce1–S2 <sup>#3</sup>	3.2709(6)	K1–O4 <sup>#3</sup>	3.2189(19)
Ce1–O1 <sup>#2</sup>	2.5229(16)	K1–O5 <sup>#7</sup>	2.9625(18)
Ce1–O2 <sup>#4</sup>	2.4976(16)	K1–O6 <sup>#10</sup>	3.0834(18)
Ce1–O2 <sup>#2</sup>	2.5052(16)	K1–O6 <sup>#4</sup>	2.7871(17)
Ce1–O4	2.4816(16)	K1–O6 <sup>#7</sup>	2.8963(18)
Ce1–O5	2.4689(16)	K1–O8 <sup>#10</sup>	3.0998(17)
Ce1–O7 <sup>#3</sup>	2.5372(16)	S1–O1	1.4763(16)
Ce1–O7 <sup>#5</sup>	2.5143(16)	S1–O2	1.5065(16)
Ce1–O8 <sup>#6</sup>	2.5692(15)	S1–O3	1.4297(17)
Ce1–O8 <sup>#3</sup>	2.6764(16)	S1–O4	1.4778(17)
K1–S1 <sup>#3</sup>	3.5500(8)	S2–O5	1.4616(16)
K1–S2 <sup>#7</sup>	3.4867(8)	S2–O6	1.4353(17)
K1–O1	2.7430(16)	S2–O7	1.5009(16)
K1–O3 <sup>#8</sup>	2.7681(19)	S2–O8	1.5065(16)

Symmetry transformations used to generate equivalent atoms:

#1: +X, 0.5-Y, 0.5+Z; #2: -1+X, 0.5-Y, 0.5+Z; #3: +X, 0.5-Y, -0.5+Z; #4: 1-X, -Y, 1-Z;  
#5: 1-X, -0.5+Y, 0.5-Z; #6: 1-X, 1-Y, 1-Z; #7: 1+X, 0.5-Y, -0.5+Z; #8: 2-X, 1-Y, -Z;  
#9: 2-X, -Y, -Z; #10: 1+X, +Y, -1+Z; #11: -1+X, +Y, 1+Z; #12: 1-X, 0.5+Y, 0.5-Z;

**Table S7.** Bond angles [deg] for the  $P2_1/c$  phase of  $\text{KCe}(\text{SO}_4)_2$ .

Atom–Atom–Atom	Angle [°]	Atom–Atom–Atom	Angle [°]
S1–Ce1–K1	123.756(13)	O4–K1–S2	80.59(4)
S1–Ce1–S2	175.677(13)	O4–K1–O4	129.25(4)
S2–Ce1–K1	53.601(12)	O4–K1–O6	100.47(5)
O1–Ce1–K1	136.34(4)	O4–K1–O8	62.21(4)
O1–Ce1–S1	27.27(4)	O5–K1–S1	159.92(4)
O1–Ce1–S2	157.05(4)	O5–K1–S2	24.51(3)
O1–Ce1–O7	154.51(5)	O5–K1–O4	155.09(5)
O1–Ce1–O8	93.31(5)	O5–K1–O4	71.83(5)
O1–Ce1–O8	138.74(5)	O5–K1–O6	98.32(5)
O2–Ce1–K1	65.40(4)	O5–K1–O8	63.46(4)
O2–Ce1–K1	106.36(4)	O6–K1–S1	151.22(4)
O2–Ce1–S1	92.43(4)	O6–K1–S1	74.78(4)
O2–Ce1–S1	27.89(4)	O6–K1–S1	62.25(3)
O2–Ce1–S2	83.32(4)	O6–K1–S2	104.52(4)
O2–Ce1–S2	147.81(4)	O6–K1–S2	120.01(4)
O2–Ce1–O1	55.12(5)	O6–K1–S2	23.76(3)
O2–Ce1–O1	119.34(5)	O6–K1–O4	67.40(4)
O2–Ce1–O2	64.62(6)	O6–K1–O4	74.59(5)
O2–Ce1–O7	112.41(5)	O6–K1–O4	89.98(5)
O2–Ce1–O7	69.10(5)	O6–K1–O4	132.01(5)
O2–Ce1–O7	142.23(5)	O6–K1–O4	80.63(5)
O2–Ce1–O7	129.90(5)	O6–K1–O5	121.70(5)
O2–Ce1–O8	66.92(5)	O6–K1–O5	48.26(4)
O2–Ce1–O8	78.00(5)	O6–K1–O6	133.99(3)
O2–Ce1–O8	149.33(5)	O6–K1–O6	139.78(5)
O2–Ce1–O8	97.52(5)	O6–K1–O6	86.23(5)
O4–Ce1–K1	130.40(4)	O6–K1–O8	46.02(4)
O4–Ce1–S1	100.04(4)	O6–K1–O8	132.40(5)
O4–Ce1–S2	83.83(4)	O6–K1–O8	111.53(5)
O4–Ce1–O1	76.00(5)	O8–K1–S1	97.23(3)
O4–Ce1–O2	122.74(5)	O8–K1–S2	87.90(3)
O4–Ce1–O2	140.85(6)	O8–K1–O4	111.29(4)
O4–Ce1–O7	74.64(5)	Ce1–S1–K1	173.736(19)
O4–Ce1–O7	83.58(6)	O1–S1–Ce1	51.54(6)
O4–Ce1–O8	76.95(5)	O1–S1–K1	122.84(7)
O4–Ce1–O8	87.14(5)	O1–S1–O2	102.50(9)
O5–Ce1–K1	38.90(4)	O1–S1–O4	109.69(10)
O5–Ce1–S1	85.28(4)	O2–S1–Ce1	51.08(6)

O5–Ce1–S2	92.37(4)	O2–S1–K1	134.17(7)
O5–Ce1–O1	99.33(6)	O3–S1–Ce1	130.40(8)
O5–Ce1–O2	68.15(5)	O3–S1–K1	47.00(7)
O5–Ce1–O2	73.68(5)	O3–S1–O1	113.93(10)
O5–Ce1–O4	149.25(5)	O3–S1–O2	111.02(10)
O5–Ce1–O7	74.91(5)	O3–S1–O4	111.24(10)
O5–Ce1–O7	105.99(5)	O4–S1–Ce1	118.27(7)
O5–Ce1–O8	76.53(5)	O4–S1–K1	65.06(7)
O5–Ce1–O8	133.79(5)	O4–S1–O2	108.00(10)
O7–Ce1–K1	81.09(4)	Ce1–S2–K1	176.633(19)
O7–Ce1–K1	69.00(4)	Ce1–S2–K1	79.974(15)
O7–Ce1–S1	151.69(4)	K1–S2–K1	103.30(2)
O7–Ce1–S1	92.15(4)	O5–S2–Ce1	120.25(7)
O7–Ce1–S2	90.74(4)	O5–S2–K1	57.23(7)
O7–Ce1–S2	26.27(4)	O5–S2–K1	147.56(7)
O7–Ce1–O1	73.57(5)	O5–S2–O7	108.20(10)
O7–Ce1–O7	115.69(4)	O5–S2–O8	111.51(9)
O7–Ce1–O8	150.83(5)	O6–S2–Ce1	128.01(7)
O7–Ce1–O8	65.66(5)	O6–S2–K1	54.39(7)
O7–Ce1–O8	66.97(5)	O6–S2–K1	56.49(7)
O7–Ce1–O8	53.29(5)	O6–S2–O5	111.61(10)
O8–Ce1–K1	43.30(3)	O6–S2–O7	112.42(10)
O8–Ce1–K1	123.46(4)	O6–S2–O8	110.48(10)
O8–Ce1–S1	154.17(3)	O7–S2–Ce1	48.44(6)
O8–Ce1–S1	86.35(4)	O7–S2–K1	129.23(7)
O8–Ce1–S2	27.06(3)	O7–S2–K1	104.12(6)
O8–Ce1–S2	92.69(4)	O7–S2–O8	102.27(9)
O8–Ce1–O8	119.48(4)	O8–S2–Ce1	53.91(6)
S2–K1–S1	173.64(2)	O8–S2–K1	57.60(6)
O1–K1–S1	81.43(4)	O8–S2–K1	128.51(7)
O1–K1–S2	92.51(4)	Ce1–O1–K1	117.66(6)
O1–K1–O3	77.06(5)	S1–O1–Ce1	101.19(8)
O1–K1–O3	96.94(5)	S1–O1–K1	136.66(9)
O1–K1–O4	136.01(5)	Ce1–O2–Ce1	115.38(6)
O1–K1–O4	61.63(5)	S1–O2–Ce1	143.29(9)
O1–K1–O5	114.96(5)	S1–O2–Ce1	101.03(8)
O1–K1–O6	119.91(5)	K1–O3–K1	100.03(5)
O1–K1–O6	65.20(5)	S1–O3–K1	110.90(10)
O1–K1–O6	70.92(5)	S1–O3–K1	139.40(11)
O1–K1–O8	161.56(5)	Ce1–O4–K1	103.74(6)

O3–K1–S1	97.48(4)	K1–O4–K1	86.46(4)
O3–K1–S1	22.10(4)	S1–O4–Ce1	131.80(10)
O3–K1–S2	163.27(4)	S1–O4–K1	90.34(8)
O3–K1–S2	79.16(4)	S1–O4–K1	114.27(8)
O3–K1–O3	116.39(5)	Ce1–O5–K1	109.55(6)
O3–K1–O4	78.92(5)	S2–O5–Ce1	145.97(10)
O3–K1–O4	46.45(5)	S2–O5–K1	98.26(8)
O3–K1–O4	83.02(5)	K1–O6–K1	138.10(6)
O3–K1–O4	141.78(5)	K1–O6–K1	93.77(5)
O3–K1–O5	76.38(5)	K1–O6–K1	92.63(5)
O3–K1–O5	147.90(5)	S2–O6–K1	100.67(8)
O3–K1–O6	142.13(5)	S2–O6–K1	137.88(10)
O3–K1–O6	153.79(5)	S2–O6–K1	101.85(8)
O3–K1–O6	66.43(5)	Ce1–O7–Ce1	116.37(6)
O3–K1–O6	84.27(5)	S2–O7–Ce1	105.29(8)
O3–K1–O6	63.60(5)	S2–O7–Ce1	138.22(9)
O3–K1–O6	67.57(5)	Ce1–O8–Ce1	109.81(6)
O3–K1–O8	87.46(5)	Ce1–O8–K1	100.40(5)
O3–K1–O8	84.93(5)	Ce1–O8–K1	106.37(5)
O4–K1–S1	105.12(4)	S2–O8–Ce1	137.38(9)
O4–K1–S1	24.60(3)	S2–O8–Ce1	99.04(8)
O4–K1–S2	149.25(3)	S2–O8–K1	98.17(8)
Ce1–O4–K1	112.45(6)		

Symmetry transformations used to generate equivalent atoms:

#1: +X, 0.5–Y, 0.5+Z; #2: -1+X, 0.5–Y, 0.5+Z; #3: +X, 0.5–Y, -0.5+Z; #4: 1–X, -Y, 1–Z; #5: 1–X, -0.5+Y, 0.5–Z; #6: 1–X, 1–Y, 1–Z; #7: 1+X, 0.5–Y, -0.5+Z; #8: 2–X, 1–Y, -Z; #9: 2–X, -Y, -Z; #10: 1+X, +Y, -1+Z; #11: -1+X, +Y, 1+Z; #12: 1–X, 0.5+Y, 0.5–Z;

**Table S8.** The thermal stability, birefringent variation and number of cycles of the reported materials caused by phase transitions.

Compound	thermal stability / °C	birefringent variation / %	number of cycles
Eu <sub>2</sub> [SiO <sub>4</sub> ] <sup>7</sup>	297	168	≤1
BaGa <sub>4</sub> Se <sub>7</sub> <sup>8</sup>	968	129	≤1
K <sub>2</sub> TeW <sub>3</sub> O <sub>12</sub> <sup>9</sup>	800	102	≤1
BaMo <sub>3</sub> O <sub>10</sub> <sup>10</sup>	800	51	≤1
SrCu <sub>2</sub> SnS <sub>4</sub> <sup>11</sup>	900	23	≤1
( <i>N</i> -methylcyclohexylammonium) <sub>2</sub> PbCl <sub>4</sub> <sup>12</sup>	247	400	≤1
[(CH <sub>3</sub> ) <sub>2</sub> CH(CH <sub>2</sub> ) <sub>2</sub> NH <sub>3</sub> ] <sub>2</sub> (CH <sub>3</sub> NH <sub>3</sub> ) <sub>2</sub> Pb <sub>3</sub> Cl <sub>10</sub> <sup>13</sup>	237	/	≤1
[Ag(NH <sub>3</sub> ) <sub>2</sub> ] <sub>2</sub> SO <sub>4</sub> <sup>14</sup>	150	34	≤1
(C <sub>2</sub> N <sub>3</sub> H <sub>4</sub> ) <sub>2</sub> PbCl <sub>4</sub> <sup>15</sup>	257	20	6
<b>This work</b>	<b>810</b>	<b>50</b>	<b>10</b>

**Table S9.** Local dipole moment calculation for the  $P\bar{1}$  phase of  $\text{KCe}(\text{SO}_4)_2$ .

Species	dipole moment			magnitude	
	x	y	z	deby	esu·cm/ $\text{\AA}^3$
CeO <sub>9</sub>	-8.264	-2.151	-1.544	17.588	0.110
KO <sub>10</sub>	-8.532	0.933	0.942	17.184	0.108
S(1)O <sub>4</sub>	-1.384	-1.898	1.141	5.135	0.032
S(2)O <sub>4</sub>	0.644	-0.258	2.182	4.579	0.029

**Table S10.** Local dipole moment calculation for the  $P2_1/c$  phase of  $\text{KCe}(\text{SO}_4)_2$ .

Species	dipole moment			magnitude	
	$x$	$y$	$z$	deby	$\text{esu}\cdot\text{cm}/\text{\AA}^3$
$\text{CeO}_9$	-2.361	-1.712	1.432	13.182	0.079
$\text{KO}_{10}$	1.067	-1.335	-3.648	16.285	0.098
$\text{S}(1)\text{O}_4$	-2.576	0.837	-1.407	11.995	0.072
$\text{S}(2)\text{O}_4$	1.880	-0.018	1.118	8.575	0.052

**Figure S1.** The fundamental building unit of the (a)  $P\bar{1}$  phase of  $\text{KCe}(\text{SO}_4)_2$  and the [Ce-S-O] chain of the (b)  $P2_1/c$  phase of  $\text{KCe}(\text{SO}_4)_2$ .

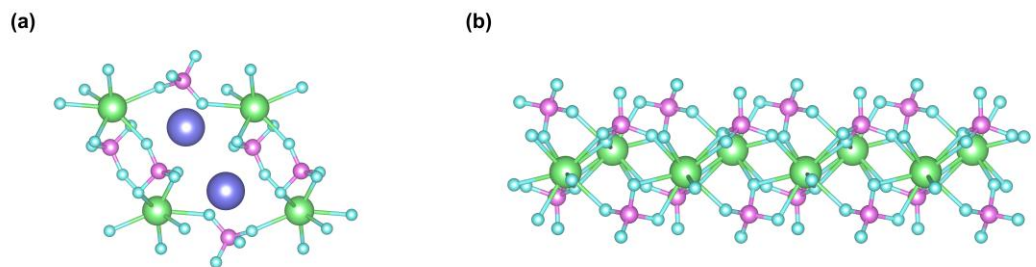


**Figure S2.** The *in-situ* variable-temperature PXRD patterns of  $P\bar{1}$ - $\text{KCe}(\text{SO}_4)_2$ .

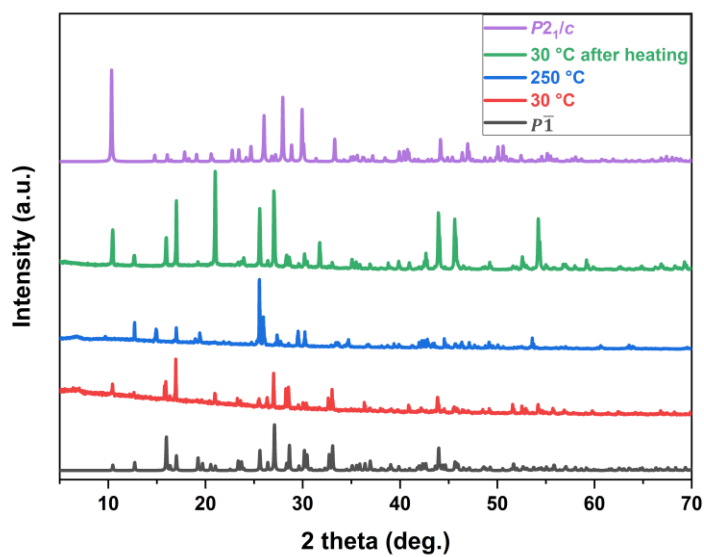


**Figure S3.** The elemental analysis results for the  $P\bar{1}$  phase and  $P2_1/c$  phase of  $KCe(SO_4)_2$ .

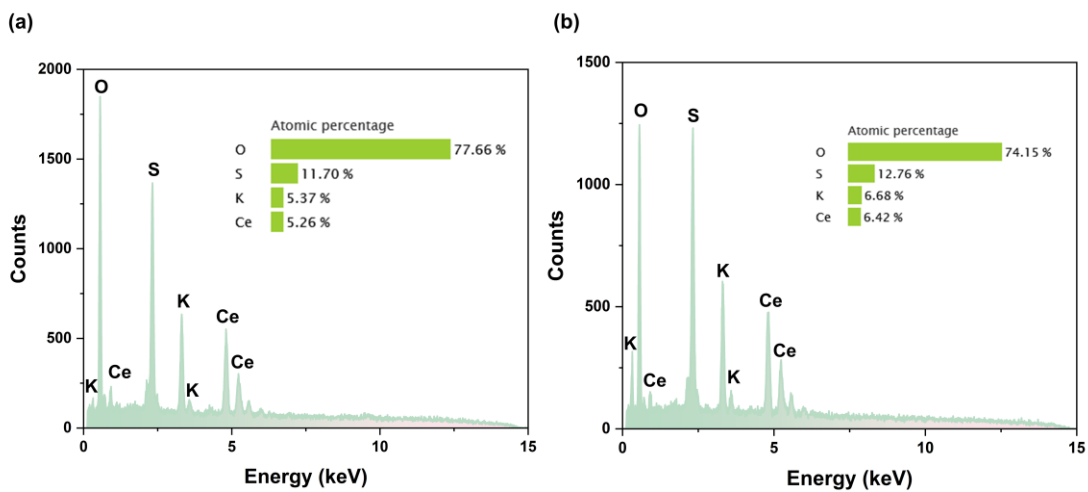


**Figure S4.** IR Spectra of (a)  $P\bar{1}$  phase and (b)  $P2_1/c$  phase of  $\text{KCe}(\text{SO}_4)_2$ .

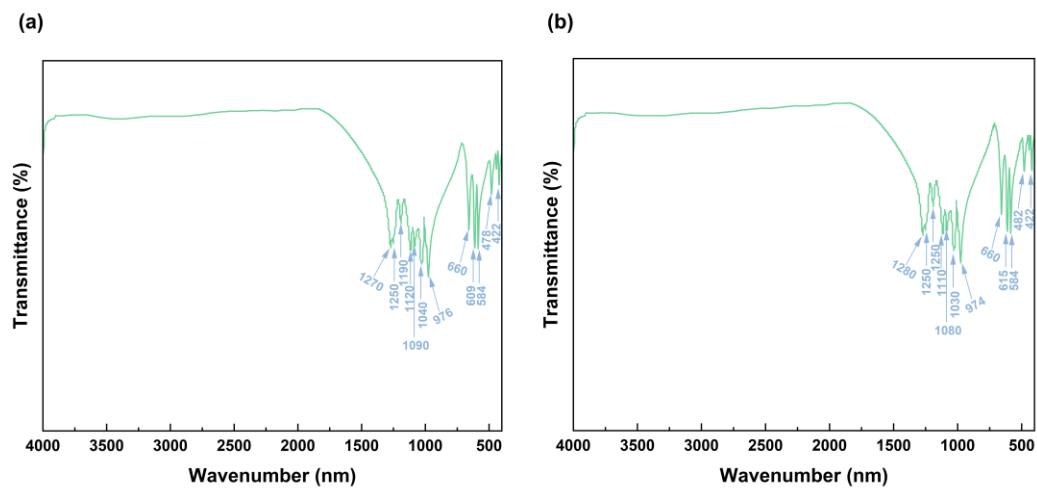


**Figure S5.** UV-vis-NIR diffuse reflectance spectra of (a)  $P\bar{1}$  phase and (b)  $P2_1/c$  phase of  $\text{KCe}(\text{SO}_4)_2$ .

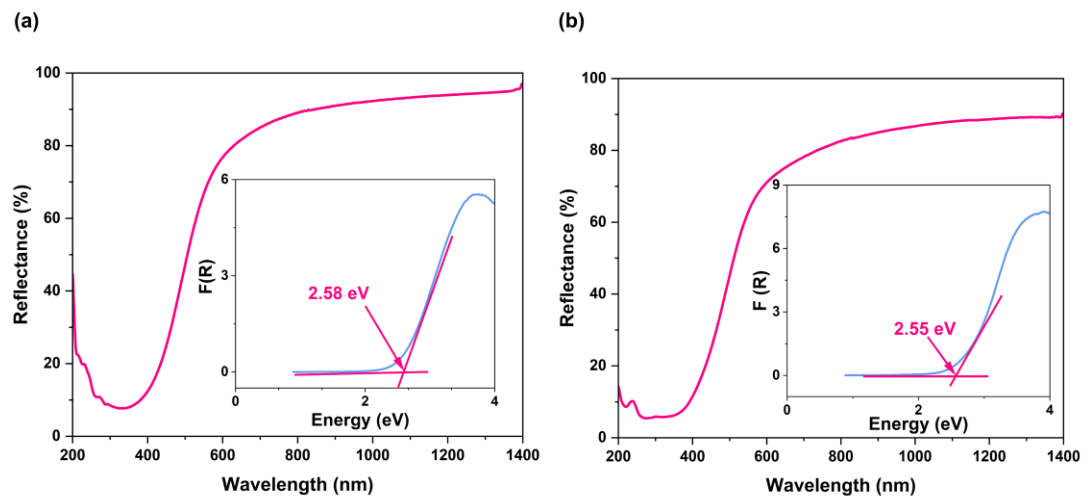


**Figure S6.** The calculated and experimental values of birefringence of (a)  $P\bar{1}$  phase and (b)  $P2_1/c$  phase of  $\text{KCe}(\text{SO}_4)_2$ .

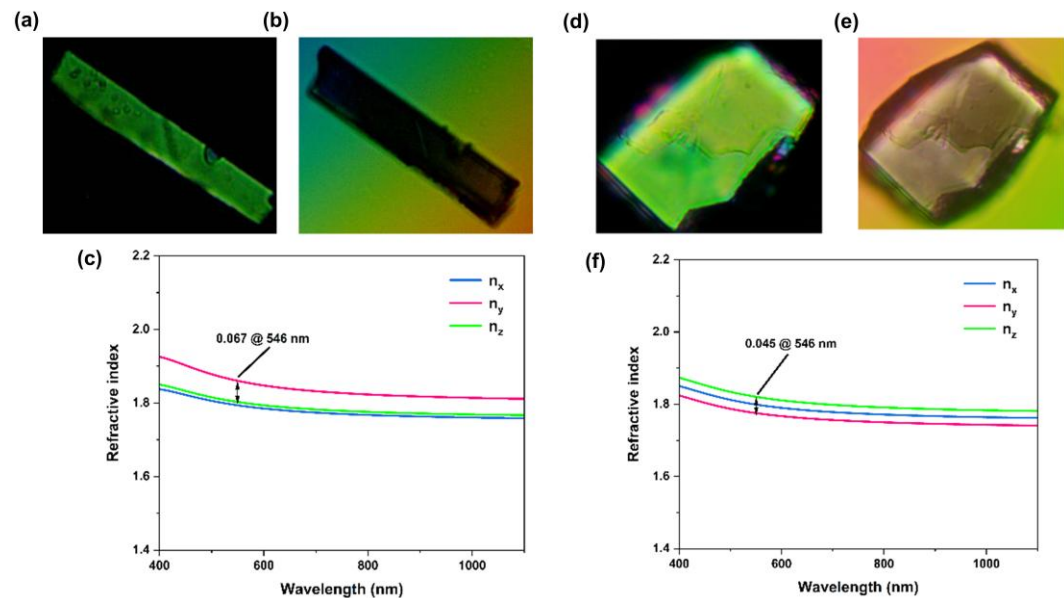


**Figure S7.** The measurement of thickness of (a)  $P\bar{1}$  phase and (b)  $P2_1/c$  phase of  $KCe(SO_4)_2$ .

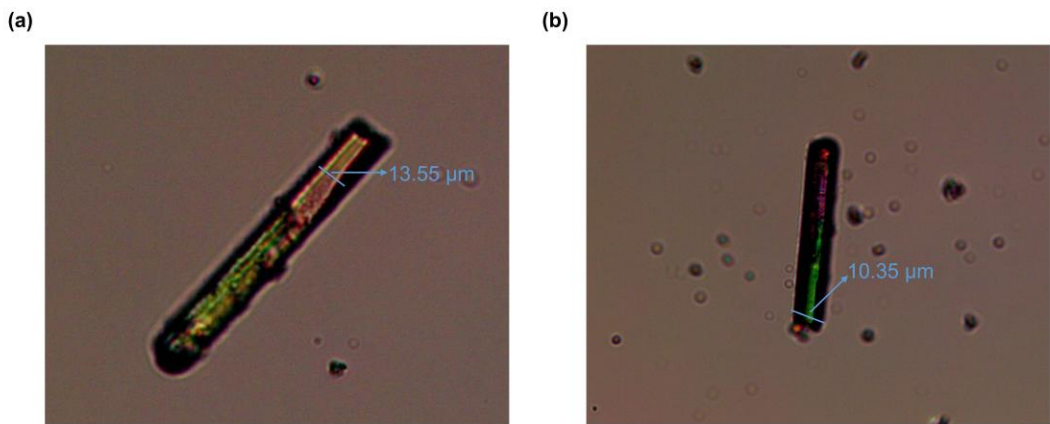


**Figure S8.** Comparison of (a) original and (b) achieved extinction images of the crystal after the phase transition of  $P\bar{1}$  - $\text{KCe}(\text{SO}_4)_2$ .

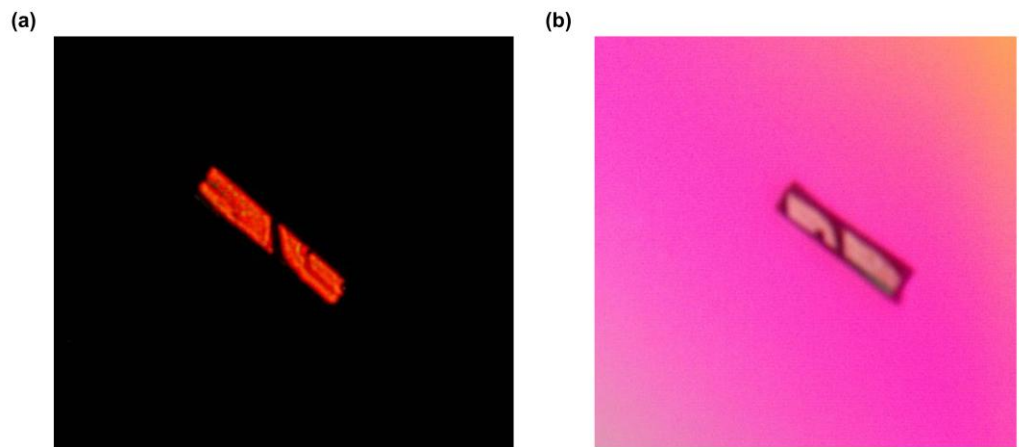
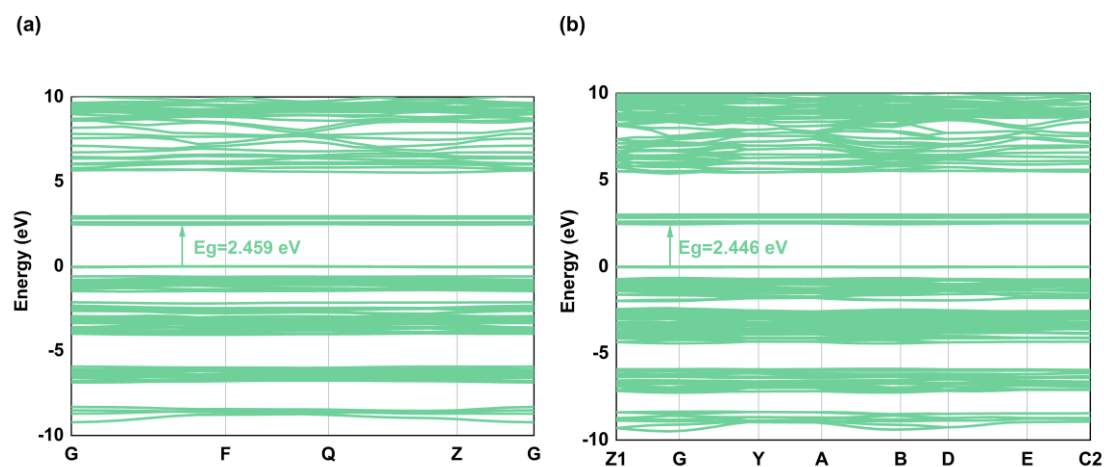


**Figure S9.** The calculated band gaps of (a)  $P\bar{1}$  phase and (b)  $P2_1/c$  phase of  $KCe(SO_4)_2$ .



## Refenence

1. O. V. Dolomanov; L. J. Bourhis; R. J. Gildea; J. A. K. Howard and H. Puschmann, OLEX2: a complete structure solution, refinement and analysis program. *J. Appl. Crystallogr.*, **2009**, *42*, 339-341.
2. A. L. Spek, Single-crystal structure validation with the program PLATON. *J. Appl. Cryst.*, **2003**, *36*, 7-13.
3. Stewart J. C.; Matthew D. S.; Chris J. P.; Phil J. H.; Matt I. J. P.; Keith R. and Mike C. P., First principles methods using CASTEP. *Z. Kristall.*, **2005**, *220*, 567–570.
4. J. S. Lin; A. Qteish; M. C. Payne and V. Heine, Optimized and transferable nonlocal separable ab initio pseudopotentials. *Phys. Rev. B.*, **1993**, *47*, 4174-4180.
5. A. M. Rappe ; K. M. Rabe ; E. Kaxiras and J. D. Joannopoulos, Optimized pseudopotentials. *Phys. Rev. B.*, **1990**, *41*, 1227-1230.
6. Z. S. Lin; X. X. Jiang; L. Kang; P. F. Gong; S. Y. Luo and Ming-Hsien. Lee, First-principles materials applications and design of nonlinear optical crystals. *J. Phys. D.,Appl. Phys.*, **2014**, *47*, 253001.
7. C. Funk; J. Köhler; I. Lazar; D. Kajewski; K. Roleder; J. Nuss; A. Bussmann-Holder; H. Bamberger; J. van Slageren; D. Enseling; T. Jüstel and T. Schleid, Old and New Insights into Structure and Properties of Eu<sub>2</sub>[SiO<sub>4</sub>]. *Cryst. Growth Des.*, **2018**, *18*, 6316-6325.
8. L. Isaenko; L. F. Dong; S. V. Melnikova; M. S. Molokeev; K. E. Korzhneva; P. G. Krinitin; A. F. Kurus; D. A. Samoshkin; R. A. Belousov and Z. S. Lin, Phase Transitions and Nonlinear Optical Property Modifications in BaGa<sub>4</sub>Se<sub>7</sub>. *Inorg. Chem.*, **2024**, *63*, 10042-10049.
9. M. Chen; Z. L. Liang; Y. Shui; B. X. Li; X. X. Jiang; Z. S. Lin and H. M. Liu, Second Harmonic Generation in β-K<sub>2</sub>TeW<sub>3</sub>O<sub>12</sub>: An Acentric Crystal Designed from Centric Phase via Pressure Modulation. *Inorg. Chem.*, **2024**, *63*, 12894-12900.
10. X. Y. Long; R. An; Y. Lv; X. Y. Wu and M. Mutailipu, BaMo<sub>3</sub>O<sub>10</sub> Polymorphs with Tunable Symmetries and Properties. *Inorg. Chem.*, **2023**, *62*, 10059-10063.
11. Y. Yang; K. Wu; B. B. Zhang; X. W. Wu and M. H. Lee, Infrared Nonlinear Optical Polymorphs α- and β-SrCu<sub>2</sub>SnS<sub>4</sub> Exhibiting Large Second Harmonic Generation Responses with Requisite Phase-Matching Behavior. *Chem. Mat.*, **2020**, *32*, 1281-1287.
12. Y. Ma; B. B. Wang; W. J. Li; Y. Liu; W. Q. Guo; H. J. Xu; L. W. Tang; Q. S. Fan; J. H. Luo and Z. H. Sun, Unusual Triple-State Switching of Thermally Induced Birefringence in a Two-Dimensional Perovskite Ferroelectric. *J. Am. Chem. Soc.*, **2024**, *146*, 27287-27292.
13. J. Q. Wang; Y. Ma; Z. J. Wang; X. T. Liu; S. G. Han; Y. Liu; W. Q. Guo; J. H. Luo and Z. H. Sun, Unusual ferroelectric-dependent birefringence in 2D trilayered perovskite-type ferroelectric exploited by dimensional tailoring. *Matter*, **2022**, *5*, 194-205.
14. Y. C. Yang; X. Liu; X. B. Deng; L. M. Wu and L. Chen, Hydrogen Bond-Driven Order–Disorder Phase Transition in the Near-Room-Temperature Nonlinear Optical Switch [Ag(NH<sub>3</sub>)<sub>2</sub>]<sub>2</sub>SO<sub>4</sub>. *J. Am. Chem. Soc.*, **2022**, *2*, 2059-2067.
15. Z. Y. Wang; X. Chen; Y. P. Song; Z. P. Du; Y. Zhou; M. J. Li; W. Q. Huang; Q. T. Xu; Y. Q. Li; S. G. Zhao and J. H. Luo, A Two-Dimensional Hybrid Perovskite With

Heat Switching Birefringence. Angew. Chem., Int. Ed., **2023**, *62*, e202311086.